Phason and Amplitudon in the Charge-Density-Wave Phase of One-Dimensional Charge Stripes in $La_{2-x}Sr_xCuO_4$

S. Sugai, Y. Takayanagi, and N. Hayamizu
Department of Physics, Faculty of Science, Nagoya University, Furo-cho, Chikusa-ku, Nagoya 464-8602, Japan
(Received 17 December 2005; published 6 April 2006)

The present systematic Raman scattering experiments reveal the phason and amplitudon of the charge density wave (CDW) mode in the charge stripes of $La_{2-x}Sr_xCuO_4$. Only about 15% of the electronic density of states condenses into the CDW state. The symmetries of the CDW modes change by the rotation of the stripes at the insulator-metal transition. The energy of the phason is finite at $0.06 \leq x \leq 0.1$ and zero at $x = 0.035$ and $0.115 \leq x \leq 0.135$, which suggests that the CDW is commensurate at $0.06 \leq x \leq 0.1$ and incommensurate otherwise. The zero-energy phason seems to reduce T_c at $x = 1/8$.

DOI: 10.1103/PhysRevLett.96.137003 PACS numbers: 74.72.Dn, 71.45.Lr, 72.15.Nj, 78.30.−j

The formation of spin-charge stripes in $La_{2-x}Sr_xCuO_4$ (LSCO) is one of the intriguing phenomena in high T_c superconductors. The dynamics of charge stripes perpendicular to them has been stressed to cause the metallic properties. However, an isolated one-dimensional (1D) conductor inevitably changes into an insulator at low temperatures because of the localization [1] and the formation of the charge density wave (CDW) below the transition temperature (T_{CDW}). If CDW along the stripe is found, it comes to give an answer to the long-standing problem that in LSCO the T_c is low and the superconducting gap energy is small in comparison with other high T_c superconductors.

The stripes are related to a small drop of T_c and almost complete suppression of T_c at $x = 1/8$ in LSCO and $La_{2-x}Ba_xCuO_4$ (LBCO), respectively [2,3]. Neutron scattering disclosed the spatially modulated dynamical spin correlations as magnetic peaks at $(\pi \pm 2\pi\delta, \pi)$ and $(\pi, \pi \pm 2\pi\delta)$ [4–11]. Tranquada *et al.* [6] showed that in $La_{1.48}Nd_{0.4}Sr_{0.12}CuO_4$ spin stripes and charge stripes are created below T_{ss} and T_{cs}, respectively. The antiferromagnetically ordered spin stripes are periodically separated by charge stripes in the CuO_2 plane. The spin stripe includes three Cu atoms and the charge stripe includes one Cu atom in width. Further neutron scattering experiments found that the direction of the stripes rotates from the vertical (parallel) to diagonal direction to the Cu-O-Cu axes, as the carrier density decreases from the metallic phase ($x \geq 0.06$) to the insulating phase ($x \leq 0.05$) in LSCO [10,11]. The inter-charge-stripe distance decreases as $d = a/2x$ with the increase of carrier density below $x = 0.12$ and then becomes constant above it [8]. Figure 1 shows the charge and spin stripes in the insulating phase at $x = 0.035$ and in the metallic underdoped phase at $x = 0.06$. The interstripe distance is large in the low doping region and the charge stripe may be considered as an isolated 1D chain.

In the CDW phase an energy gap (E_{CDW}) is created at the Fermi energy (E_F) by the modulation of the lattice at $2k_F$. Therefore, the metallic state cannot be produced by the simple 1D conducting stripes. Two models are considered to cause the metallic state at low temperatures. One is the mixed phase of the 1D insulating stripe region and the two-dimensional (2D) metallic region in real space and the other is the mixed phase in k space. The former model is removed from the Fermi surface (FS) observed by angle-resolved photoemission spectroscopy (ARPES) [12–15]. ARPES observed the very strong FS called Fermi arc near $(\pi/2, \pi/2)$ as shown in the lower panels of Fig. 1 [12,14]. The Fermi surfaces of the charge stripes are shown by the straight lines. ARPES did not observe the dotted lines in the metallic phase. Thus the insulating 1D charge stripes and the metallic 2D region are separated in k space in the metallic phase. In the insulating phase the present experimental result is consistent with the model shown in Fig. 1(a). The 1D FS coexists with the 2D FS (Fermi arc) near $(\pi/2, \pi/2)$ below T_{cs}. Electronic excitations near the

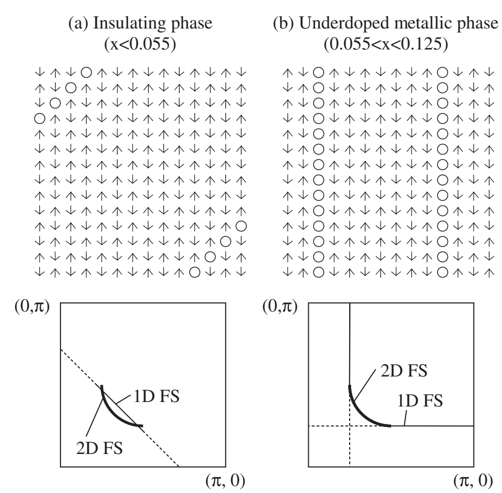

FIG. 1. Spin-charge stripe structure below T_{cs} in (a) the insulating phase ($x = 0.035$) and (b) the underdoped metallic phase ($x = 0.06$). Charges and spins are shown by the open circles and arrows, respectively. Lower panels are Fermi surfaces of the 2D quasiparticles and the 1D charge stripes. The dotted lines are missing in ARPES.

FS around $(\pi, 0)$ and $(\pi/2, \pi/2)$ are observed in the B_{1g} and B_{2g} spectra, respectively [16]. Therefore, the Raman scattering from 1D FS below T_{cs} changes from B_{2g} in the insulating phase to B_{1g} in the metallic phase, while the symmetry of the scattering from 2D FS is B_{2g} in both insulating and metallic phases at all temperatures.

Tassini *et al.* [17] reported the Raman study from the charge stripes on the assumption that the stripes exist below room temperature and the temperature dependence results from only the stripes. Based on the assumption they stressed that the temperature-dependent Drude-like peak in the B_{2g} Raman susceptibility at $x = 0.02$ changed to the B_{1g} susceptibility at $x = 0.1$ by the rotation of the stripes. Raman susceptibility is the Raman spectra divided by $n(\omega, T) + 1$, where $n(\omega, T)$ is the Bose-Einstein statistical factor. Their assumption, however, contradicts with the neutron scattering [7,9,10], nuclear quadrupole resonance (NQR) [18], and ARPES [12,14]. The onset temperatures of the stripe structure are $T_{ss} = 18$ K [10] at $x = 0.03$ and 40 K [7] and 32 K [9] at $x = 0.12$. Only below T_{cs} which is a little higher than T_{ss}, the spectra from the stripes should be observed. Above T_{cs} there exists only 2D FS which gives B_{2g} scattering in both insulating and metallic phases. Therefore, the B_{2g} spectra at $x = 0.02$ must not resemble the B_{1g} spectra at $x = 0.1$ above T_{cs}. Their observed temperature dependence is an artifact produced by the expression in the Raman susceptibility. The gradient of the initial slope of the Raman susceptibility always decreases as temperature increases, which causes the low-energy peak in the differential susceptibility between two temperatures.

In the present experiment the 1D response is obtained by the CDW energy gap and the collective CDW modes, the phase mode (phason) and the amplitude mode (amplitudon) [19]. These collective modes are coupled charge-phonon modes which are folded from $-2k_F$ and $2k_F$ to $k = 0$. The phason has the dispersion like an acoustic phonon mode ($\omega = 0$ at $k = 0$) in the incommensurate CDW phase. In the commensurate CDW phase (the wavelength of the CDW is a rational number times the lattice constant) the phason has a finite energy at $k = 0$ due to the locking by the lattice potential [19]. Therefore, the phason is identified, if the distinction of the energy, zero or finite, coincides with the commensurability, incommensurate or commensurate.

Single crystals were synthesized by a traveling-solvent floating-zone method in an infrared radiation furnace. The superconducting transition temperatures are 13 K ($x = 0.06$), 27 K (0.08), 33 K (0.1), 33 K (0.115), 36 K (0.125), 39 K (0.135), and 42 K (0.15). Raman scattering was executed on fresh cleaved surfaces in a quasiback-scattering configuration with 5145 Å Ar-ion laser light. The tetragonal notation is used for the symmetry of the spectra. The B_{1g} and B_{2g} spectra are observed in the (xy) and (ab) polarization configurations, respectively. (xy) denotes that the polarization of incident (scattered) light is parallel to the x (y) direction. The a and b axes are the directions along the Cu-O-Cu axes and the x and y directions are $(\vec{a} + \vec{b})/\sqrt{2}$ and $(-\vec{a} + \vec{b})/\sqrt{2}$.

Figures 2(a)–2(c) show the raw B_{2g} Raman spectra and Figs. 2(a′)–2(c′) show the Raman susceptibility. Figures 2(d)–2(k) show the raw B_{1g} Raman spectra. Raman scattering includes various temperature-dependent components. Bosonic excitations like the phason, amplitudon, and phonons have the temperature dependence of $n(\omega, T) + 1$, while the electronic transition between two states with Fermi-Dirac statistical factor is not propor-

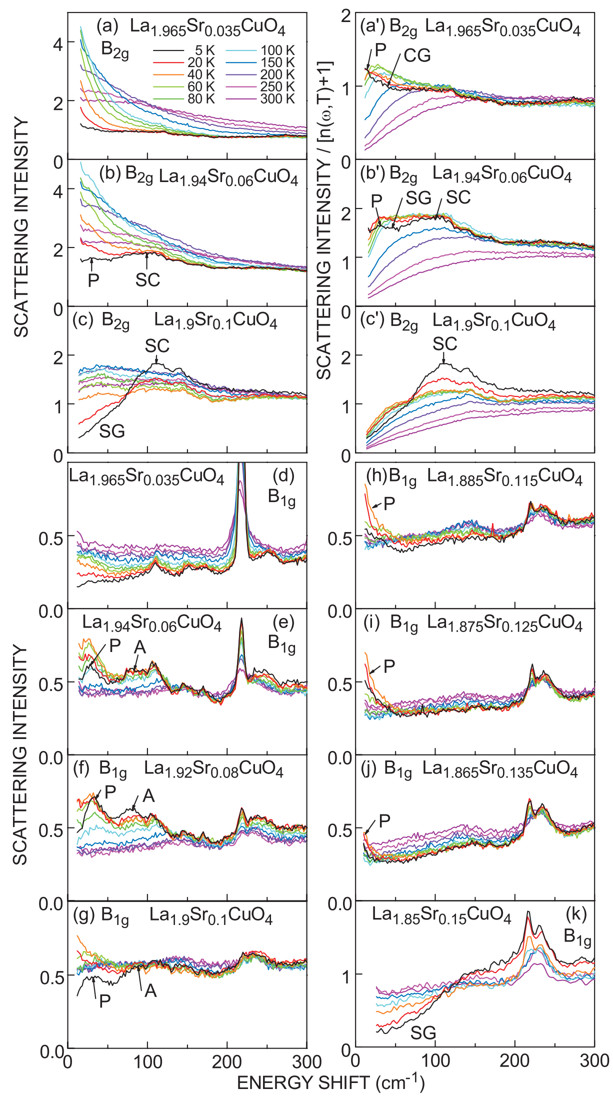

FIG. 2 (color). (a)–(c) B_{2g} raw Raman spectra in the insulating phase ($x = 0.035$) and the metallic phase ($x = 0.06$ and 0.01). The increase of the low-energy intensity with narrowing as temperature decreases from 300 K to 100 K near the insulator-metal transition ($x = 0.055$) is due to the development of the quasiparticle peak. The decrease of the intensity below 100 K is due to the formation of the pseudogap. (a′)–(c′) B_{2g} Raman susceptibility obtained from the raw Raman spectra divided by $n(\omega, T) + 1$. (d)–(k) B_{1g} raw Raman spectra. CG: CDW gap, SG: superconducting gap, SC: superconducting coherence peak, P: phason, A: amplitudon.

tional to $n(\omega, T) + 1$. Furthermore, almost temperature-independent electronic scattering is often observed in high T_c superconductors. The possible origins are the marginal Fermi liquid [20] or nested Fermi surfaces [21]. Figures 2(a′)–2(c′) are plotted for the comparison between the two plotting methods.

The B_{2g} scattering intensity increases from $x = 0$ to the insulator-metal transition point ($x \sim 0.055$) and then decreases with the increase of the carrier density, while the B_{1g} scattering intensity increases as the carrier density increases above $x = 0.15$ [22–24]. In the B_{2g} spectra [Fig. 2(a)] at $x = 0.035$ in the insulating phase the height of the low-energy peak centered at energy zero increases with narrowing as temperature decreases from 300 K to 100 K and then decreases in intensity below 100 K. A similar temperature dependence is also observed in the spectra [Fig. 2(b)] at $x = 0.06$ in the metallic phase. The B_{2g} low-energy scattering is caused by the intraband excitation in the quasiparticle band near $(\pi/2, \pi/2)$ which is called the Fermi arc [12,14]. The rapid increase from 300 K to 100 K is caused by the growth of the quasiparticle peak at the insulator-metal transition and the decrease below 100 K is due to the formation of the pseudogap [25–27]. The temperature dependence is observed in a different way, when it is plotted by the Raman susceptibility. At $x = 0.035$ [Fig. 2(a′)] the intensity increases toward low energy as temperature decreases from 300 K to 60 K and then the intensity decreases below 90 cm^{-1} at 40 K. The T_{ss} at $x = 0.03$ is 18 K [10]. The charge stripe is formed at a little higher temperature than T_{ss} [6]. Therefore, the decrease of intensity at 40 K is caused by the formation of the charge stripe with $E_{CDW} =$ 90 cm^{-1}. The decrease of the intensity between 60 K and 5 K is about 15% at 50 cm^{-1}. About 15% of the density of states around $(\pi/2, \pi/2)$ is used to form the charge stripes and the remainder is retained in the 2D states below T_{cs}. The increase of the intensity toward zero energy at 5 K is assigned to the phason with zero energy. At $x = 0.06$ [Fig. 2(b′)] the intensity decreases below 70 cm^{-1} as temperature decreases from 20 K to 5 K. The decrease is due to the superconducting gap, because the T_c is 13 K. The 100 cm^{-1} peak is the superconducting coherence peak. The T_{CDW} is 150 K, when it is estimated from the emergence of the phason in the B_{1g} spectra as discussed below. The decrease of the B_{2g} scattering intensity below T_{CDW} is not clearly observed, because the intensity continues to increase toward 100 K by the development of the quasiparticle band. The superconducting gap structure is clearly observed at $x = 0.1$ in Figs. 2(c) and 2(c′).

The B_{1g} spectra are very different from the B_{2g} spectra. In the insulating phase at $x = 0.035$ the intensity of the B_{1g} spectra [Fig. 2(d)] is much lower than that of B_{2g} [Fig. 2(a)] and the low-energy scattering intensity does not increase with decreasing temperature. The peaks at 110, 151, 170, 218, and 251 cm^{-1} are phonon peaks. At $x = 0.06$ the spectra are almost the same from 300 K to 150 K. Below 150 K new peaks emerge at 28 and 80 cm^{-1} (at 5 K). The peak at 108 cm^{-1} (at 5 K) is the phonon peak which is observed at $x = 0.035$. The selection rule of the CDW modes changes at the insulator-metal transition by the rotation of the stripe direction by 45°. The 28 cm^{-1} peak is assigned to the phason and the 80 cm^{-1} peak is assigned to the amplitudon. The finite energy of the phason indicates that the CDW is commensurate, consistent with the hole density, 0.5 holes/Cu, in the chain estimated by neutron scattering [8]. The intensity of the phason and amplitudon increases from $x = 0.06$ to 0.08 and then decreases to 0.1. At $x = 0.1$ the phason energy is less than the present experimental limit of 12 cm^{-1} at 40 and 20 K and becomes 28 cm^{-1} at 5 K. At $x = 0.115$ in Fig. 2(h) the phason peak emerges below 60 K. The energy is less than the experimental limit of 12 cm^{-1}. The energy is assumed to be zero, because the intercharge stripe distance is approaching a constant value (4 times the Cu-Cu distance) and the CDW becomes incommensurate [8]. The energy region of the zero-energy phason tail becomes lower and lower as the carrier density increases from $x = 0.115$ to 0.135. At $x =$ 0.15 (optimum doping) [Fig. 2(k)] the electronic scattering intensity rapidly increases and changes to produce the superconducting gap structure. No sign of the phason is observed at $x = 0.15$. Thus in the underdoped metallic phase ($0.06 \le x \le 0.135$) the temperature-dependent electronic scattering such as the development of the quasiparticle band and the formation of the superconducting gap structure is observed only in the B_{2g} spectra. The phason and the amplitudon are observed also in the B_{2g} spectra at $0.06 \le x \le 0.1$.

Figure 3(a) shows the energy of the phason and amplitudon and Fig. 3(b) shows the hole density estimated from the intercharge stripe distance measured by neutron scattering. The hole density changes from incommensurate $0.7(= 0.5 \times \sqrt{2})$/Cu at $x = 0.04$ and 0.05 in the insulating

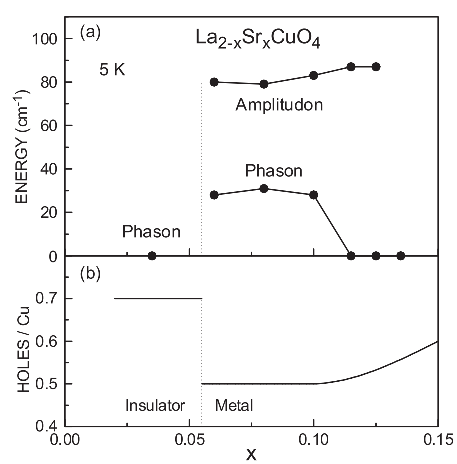

FIG. 3. (a) Carrier density dependences of the phason energy and the amplitudon energy at 5 K. (b) Hole density in the charge stripe obtained from the intercharge stripe distance measured by neutron scattering [8,11].

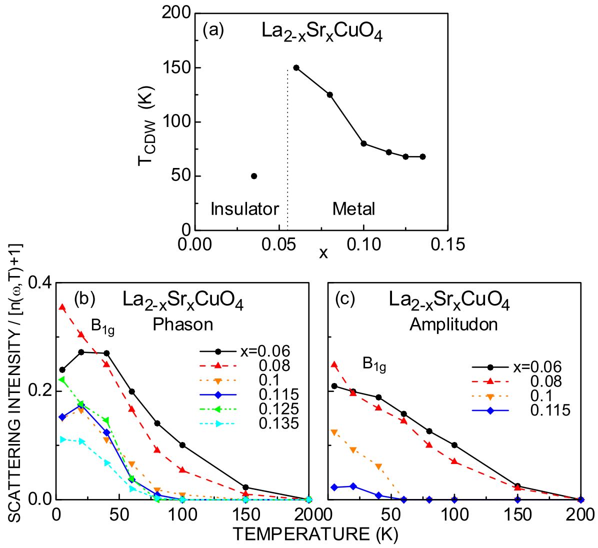

FIG. 4 (color online). (a) CDW transition temperature. (b), (c) Temperature dependence of the scattering intensity divided by $n(\omega, T) + 1$.

phase [11] to commensurate 0.5/Cu at $0.06 \leq x < 0.12$ in the metallic phase [8]. Above $x = 0.12$ the hole density increases from 0.5/Cu and becomes incommensurate, because the intercharge stripe distance becomes constant [8]. The coincidence between the phason energy, zero or finite, and the commensurability, incommensurate or commensurate, justifies the assignment of the phason. The zero phason energy at $x = 0.115$ suggests the hole density in the charge stripe is incommensurate.

Figure 4 shows (a) the T_{CDW} and the temperature-dependent intensities of (b) the phason peak and (c) the amplitudon peak. The T_{CDW} is obtained from the opening of the CDW gap at $x = 0.035$ and the onset temperature of the phason peak shown in Fig. 4(b) at $x \geq 0.6$. The T_{CDW} rapidly increases from 50 K at $x = 0.035$ to 150 K at $x = 0.06$ and then decreases to 72 K at $x = 0.115$. These temperatures are higher than $T_{ss} = 18$ K [10] at $x = 0.03$ and 40 K [7] and 32 K [9] at $x = 0.12$ obtained by neutron scattering. The T_{ss} obtained by the wipeout effects of ^{63}Cu NQR decreases monotonically from 90 K at $x = 0.07$ to 50 K at $x = 0.115$ [18]. It is known that the T_{cs} is higher than the T_{ss} [6]. It is supposed that the T_{CDW} is the same as T_{cs}, that is, the charge stripes are in the CDW state when it is produced. All the present experimental results can be interpreted in the CDW scenario.

The onset of the CDW generally makes the system insulating. In the underdoped phase the large density of states is confined into the quasiparticle state around $(\pi/2, \pi/2)$ as observed in the large, temperature-dependent B_{2g} peak at low energy. When the Fermi surfaces of the 1D charge stripes and the 2D quasiparticles are located in the same area in k space, the system becomes insulating at $x < 0.055$, even if only 15% of the density of states is distributed into the charge stripe. In the metallic region at $x > 0.055$ the Fermi surface of the 1D charge stripes is separated from that of the quasiparticles in k space as observed in the different temperature dependence between the B_{1g} and B_{2g} spectra. The zero-energy phason in the incommensurate CDW causes the decrease of conductivity and superconductivity.

In summary, we have explored the CDW modes, the phason and the amplitudon, in the charge stripe of LSCO. The component of the electronic density of states to form the CDW is only 15%. The symmetry of the phason changes from B_{2g} in the insulating phase to B_{1g} and B_{2g} in the underdoped metallic phase at $0.06 \leq x \leq 0.135$. The energy of the phason is finite at $0.06 \leq x \leq 0.1$ and zero at $x = 0.035$ and $0.115 \leq x \leq 0.135$. The zero-energy phason seems to disturb the metallic properties and reduce T_c at $x = 1/8$.

[1] E. Abrahams, P. W. Anderson, D. C. Licciardello, and T. V. Ramakrishnan, Phys. Rev. Lett. **42**, 673 (1979).
[2] K. Kumagai, Y. Nakamura, I. Watanabe, Y. Nakamichi, and H. Nakajima, J. Magn. Magn. Mater. **76–77**, 601 (1988).
[3] A. R. Moodenbaugh, Y. Xu, M. Suenaga, T. J. Folkerts, and R. N. Shelton, Phys. Rev. B **38**, 4596 (1988).
[4] S.-W. Cheong *et al.*, Phys. Rev. Lett. **67**, 1791 (1991).
[5] M. Matsuda *et al.*, Phys. Rev. B **49**, 6958 (1994).
[6] J. M. Tranquada, B. J. Sternlieb, J. D. Axe, Y. Nakamura, and S. Uchida, Nature (London) **375**, 561 (1995).
[7] T. Suzuki *et al.*, Phys. Rev. B **57**, R3229 (1998).
[8] K. Yamada *et al.*, Phys. Rev. B **57**, 6165 (1998).
[9] H. Kimura *et al.*, Phys. Rev. B **59**, 6517 (1999).
[10] S. Wakimoto *et al.*, Phys. Rev. B **60**, R769 (1999).
[11] S. Wakimoto *et al.*, Phys. Rev. B **61**, 3699 (2000).
[12] M. R. Norman *et al.*, Nature (London) **392**, 157 (1998).
[13] X. J. Zhou *et al.*, Science **286**, 268 (1999).
[14] T. Yoshida *et al.*, Phys. Rev. Lett. **91**, 027001 (2003).
[15] X. J. Zhou *et al.*, Phys. Rev. Lett. **92**, 187001 (2004).
[16] T. P. Devereaux *et al.*, Phys. Rev. Lett. **72**, 396 (1994).
[17] L. Tassini, F. Venturini, Q.-M. Zhang, R. Hackl, N. Kikugawa, and T. Fujita, Phys. Rev. Lett. **95**, 117002 (2005).
[18] A. W. Hunt, P. M. Singer, K. R. Thurber, and T. Imai, Phys. Rev. Lett. **82**, 4300 (1999).
[19] P. A. Lee, T. M. Rice, and P. W. Anderson, Solid State Commun. **14**, 703 (1974).
[20] C. M. Varma, P. B. Littlewood, S. Schmitt-Rink, E. Abrahams, and A. E. Ruckenstein, Phys. Rev. Lett. **63**, 1996 (1989).
[21] A. Virosztek and J. Ruvalds, Phys. Rev. B **42**, 4064 (1990).
[22] T. Katsufuji, Y. Tokura, T. Ido, and S. Uchida, Phys. Rev. B **48**, 16 131 (1993).
[23] J. G. Naeini, X. K. Chen, J. C. Irwin, M. Okuya, T. Kimura, and K. Kishio, Phys. Rev. B **59**, 9642 (1999).
[24] S. Sugai, H. Suzuki, Y. Takayanagi, T. Hosokawa, and N. Hayamizu, Phys. Rev. B **68**, 184504 (2003).
[25] A. Georges, G. Kotliar, W. Krauth, and M. J. Rozenberg, Rev. Mod. Phys. **68**, 13 (1996).
[26] M. Imada, A. Fujimori, and Y. Tokura, Rev. Mod. Phys. **70**, 1039 (1998).
[27] M. Yamazaki, N. Tomita, and K. Nasu, J. Phys. Soc. Jpn. **72**, 611 (2003).